



Multi-annual response of a Pampean shallow lake from central Argentina to regional and large-scale climate forcings

Lucía Guerra^{1,2} · Mateo A. Martini^{2,3} · Francisco E. Córdoba⁴ · Daniel Ariztegui¹ · Eduardo L. Piovano^{2,3}

Received: 8 May 2018 / Accepted: 20 November 2018 / Published online: 27 November 2018
© Springer-Verlag GmbH Germany, part of Springer Nature 2018

Abstract

The Pampean Plains comprise a flat area of southeastern South America (SESA), encompassing the most populated and productive area of Argentina. Several floods and droughts have been reported in the region during the last 50 years affecting lakeshore villages. In spite of the well-known importance of monitoring hydrological systems in flood-risk areas, long series of instrumental limnometric data are sparse in the Pampean Plains. Lake Melincué (33°43'S/61°28'W), located in the center of this region, provides a valuable record of the annual lake-area oscillations from 1965 to 2015. In this study we analyze the lake area variability at different time-scales, from intra-annual to multi-annual, investigating the persistence and the frequencies of the series. Our results show that the lake area oscillates following a significant quasi-bidecadal periodicity. A secondary 13 years-frequency signal was detected since the 1970s, when a dramatic increase in Lake Melincué area occurred, associated with a shift to humid conditions in SESA. The analysis of meteorological series suggests that lake area variations are controlled by precipitation and evaporation with different time-lags. Further comparisons of the lake area fluctuations with climate indices from the Pacific and Atlantic oceans provide evidence of the link between the dynamic of lakes in the Pampean Plains and both large-scale climate circulation and low-frequency phenomena. These results confirm that a regular monitoring of these shallow lake systems and the analysis of high-resolution reliable data on inland water environments of the Pampean Plains is fundamental for anticipating their hydrological responses to forecasted climate changes.

Keywords Lake area fluctuations · Shallow lake · Pampean Plains · Forcings

Electronic supplementary material The online version of this article (<https://doi.org/10.1007/s00382-018-4548-x>) contains supplementary material, which is available to authorized users.

✉ Lucía Guerra
luciaguerra83@gmail.com

¹ Department of Earth Sciences, University of Geneva, 13 rue des Maraîchers, 1205 Geneva, Switzerland

² Centro de Investigaciones en Ciencias de la Tierra (CONICET-Universidad Nacional de Córdoba), Avenida Vélez Sarsfield 1611, Córdoba X5016GCA, Argentina

³ Facultad de Ciencias Exactas, Físicas y Naturales, Universidad Nacional de Córdoba, Avenida Vélez Sarsfield 1611, Córdoba X5016GCA, Argentina

⁴ Instituto de Ecorregiones Andinas (INECOA, CONICET-UNJu), Instituto de Geología y Minería, Universidad Nacional de Jujuy, Av. Bolivia 1661, Y4600GNE San Salvador de Jujuy, Jujuy, Argentina

1 Introduction

Climate controls water availability and therefore is critical for the ecosystems in general and human population in particular that largely depend on water sources. In the Pampean Plains of Argentina, the water budget interplays with a flat terrain geomorphology, ruling the functioning of the numerous shallow lakes spread across the region. Most of these lakes and wetlands are closed and shallow hydrological systems (Iriondo 1989; Quiros and Drago 1999; Quirós et al. 2002), where vertical water interaction dominates the balance [i.e., rainfall and evaporation over lateral runoff (Zimmermann et al. 2000)]. Due to the flat landscape in which the lakes are situated relatively low-lake level fluctuations generate large areal changes. Thus, they are extremely sensitive to water balance changes, which in turn influences the physics, chemistry and biology of the lake waters and the associated sediments deposited in the lake bottom (e.g., Stutz et al. 2012; Córdoba et al. 2014; Guerra et al. 2015,

2017; Achaga et al. 2017), as well as the ecological equilibrium (Quiros and Drago 1999; Quirós et al. 2002).

Lately, changes in the regional precipitation regime have had substantial impact on water storage of the Pampean lakes in the central part of Argentina. Several studies in southeastern South America (SESA) including the Pampean Plains in central and northeastern Argentina, Uruguay, Paraguay and southern Brazil, have reported a significant precipitation increase between the 1970s and 2003 (Kayano et al. 2009; Giorgi 2002; Barros et al. 2002; Jacques-Coper and Garreaud 2015; Troin et al. 2010, 2016), and from 2013 to present. This rise in precipitation appears to be closely associated with accelerated lake expansion and is one of the most outstanding environmental events in central Argentina (Piovano et al. 2009; Leroy et al. 2010; Córdoba et al. 2014). The increase in both the area of the lakes and their water levels has generated major environmental problems in the region. As a consequence, flooding of the lake- and river-shore villages across the Pampean Plains has caused severe damages to civil infrastructure and economical activities in the most populated and productive region of Argentina (Leroy et al. 2010). Conversely, intense droughts, like the one registered between 2008 and 2012, have also a strong impact on the regional economy by reducing the crop growth and generating vast livestock mortality (Scarpati and Capriolo 2013). Numerous management initiatives on hydrological systems have been implemented along the twentieth century to both prevent and mitigate the negative effects of these extreme changes in water level. Nevertheless, their implementation requires a complete understanding of the functioning and dynamics of the regional hydroclimate.

Despite the numerous wetlands in the Pampean Plains [hundreds of lakes with surface area $> 5 \text{ km}^2$ were accounted by Quiros and Drago (1999)] and the consequences of their oscillations during the twentieth and twenty-first century, monitoring activities of their water fluctuations have been exiguous. Previous studies have already shown that satellite gridded data may provide useful information for understanding the hydrological and environmental dynamics of wetlands when instrumental series are not available (e.g., Bohn et al. 2016; Bianchi et al. 2017; Silio-Calzada et al. 2017). The integration of limnometric measurements and meteorological records with these satellite-based datasets allows a better understanding of regional hydroclimate changes as well as their frequency. Furthermore, they are critical to elucidate the triggering-mechanisms behind these hydrological shifts. Several studies addressing this subject on multiple timescales have been the focus of much research and debate around the world (IPCC 2014; Penalba et al. 2014). The robustness of these interpretations depends on the detailed analyses of reliable datasets. Previous paleoenvironmental studies have revealed that major shifts in water level of the Pampean lakes during the last millennia have been driven

by climate (Piovano et al. 2002, 2004; Stutz et al. 2012; Córdoba et al. 2014; Guerra et al. 2015, 2017; Achaga et al. 2017), while hydroclimatic simulations for SESA have predicted increasing rainfall for the forthcoming 50 years (Chou et al. 2013; IPCC 2014). The latter has a special relevance challenging the communities' ability to adapt to different water budget-scenarios.

Lake Melincué is a shallow and closed lacustrine system situated in the Santa Fe province, central Pampean Plains. The dynamics of the lake indicate a large variability conditioning the lacustrine sedimentation regimes (Guerra et al. 2017) and changes in the ecology (Romano et al. 2005, 2014). Moreover, along the twentieth century the areal increase in water distribution caused severe floods that impacted the village of Melincué as well as agricultural fields and routes generating a decrease in population (Pasotti et al. 1984; Romano et al. 2014; Peralta 2017), repeating the pattern observed at different lakeshore towns across the Pampean Plains (e.g., Córdoba et al. 2014). The latest flood was reported in May 2017 when the lake reached large parts of the city of Melincué.

Determining the frequency, cyclicity and forcings behind these hydrological changes on inland water environments of the Pampas is still an open matter that is essential for a sustainable regional development and planning. The aim of this contribution is to perform a detailed analysis of the areal changes of Lake Melincué (LM) based on a reliable data-source of hydrological information and to characterize its links to regional hydroclimate variability. Assuming that this lake behavior is a case study representative of the lake-climate interactions in the Pampean region, the focus of this study is to consider the local lake watershed within a larger-scale climatic context. Firstly, we inquire the variability of the lake areal oscillations, identifying seasonal, inter-annual and decadal signals. Subsequently, we identify the main climatic variables driving the dynamic of Lake Melincué area to understand its response to the climatic impulses at different time scales (intra-annual vs. inter-annual). Meteorological information, including standardized precipitation and temperature anomalies (SPA and STA, respectively), and a standardized precipitation index (SPEI; Harris et al. 2014) are compared with the reconstructed changes in Lake Melincué water area (LA). These results are also compared with Pacific and Atlantic oceanic indices to check for the role of this large-scale climate driver on the observed lake level oscillations. In order to disentangle natural- from human-induced changes, we also introduce a discussion about the known anthropogenic modifications of the lake watershed and their imprint on the lake area dynamics.

2 Study area

2.1 The Lake Melincué system

LM (33°43'S/61°28'W) is a shallow and closed lacustrine system, occupying an area of 84 km² (2015) within a structural depression in the eastern Pampean Plains of central Argentina, in SESA (Fig. 1a). The origin of the lake has been attributed to a structural sinking of a small block inside the main depression, and a subsequent damming of the SW–NE paleo-drainage system (Pasotti et al. 1984; Iriondo and Kröhling 2007). Aeolian loess and loessoid (Peripheral Loess Belt; Iriondo and Kröhling 2007), and palustrine sediments from the Pleistocene and Holocene (Kröhling 1999) surround the lake basin.

The lake is highly sensitive to changes in hydrology. Satellite images indicate that the surface area of LM can increase considerably after years with precipitation above average. The maximum historical water-level reached 86 m a.s.l in 2003 (Fig. 1b, c) corresponding to a water column of 7.5 m. Conversely, intervals of prolonged drought commonly lead to a retraction of the lake.

The lake system has no natural surface outlet (Fig. 1b), and thus most of the water loss occurs by evaporation. Although the original watershed comprised 1495 km², in 1940 it was separated into two subsystems as the result of an artificial channeling located almost parallel to the

northern shore of the lake (Fig. 1b). This channel, named San Urbano, was built to interrupt the northern unconfined runoff to the lake, which passed through the city of Melincué (Fig. 1b). The current LM basin comprises 678 km² and is the final collector of several intermittent wet meadows or 'cañadas' and artificial channels that drain the cultivated fields and the phreatic flow (Fig. 1b). A small stream called El Pedernal is the only permanent superficial stream feeding the lake (Fig. 1b). Even though there are no recent hydrological studies in the lake watershed, groundwater discharge constitutes a source of water to LM. Shallow groundwater inflow was inferred for the area (Kreimer 1969; Pasotti et al. 1984) and regional water table in Santa Fe province has been shown that follows the precipitation regimes (Venencio and García 2011).

The Melincué lacustrine system comprises different sedimentological sub-environments, depending on the bottom morphology (Fig. 1d). They include an external shallow marginal area with gentle slopes, which is separated by topographic heights (some of them connect to the shoreline under low lake levels) from a deeper and flat depocenter. Mudflats and ephemeral wetlands fringe the emerged littoral areas of the lake. The development and extension of these environments have fluctuated following the alternations between deep lake conditions and playa lake systems during the last 1000 years (Guerra et al. 2015).

The Melincué wetland system has been established as part of a Ramsar site (i.e. protected site in an intergovernmental

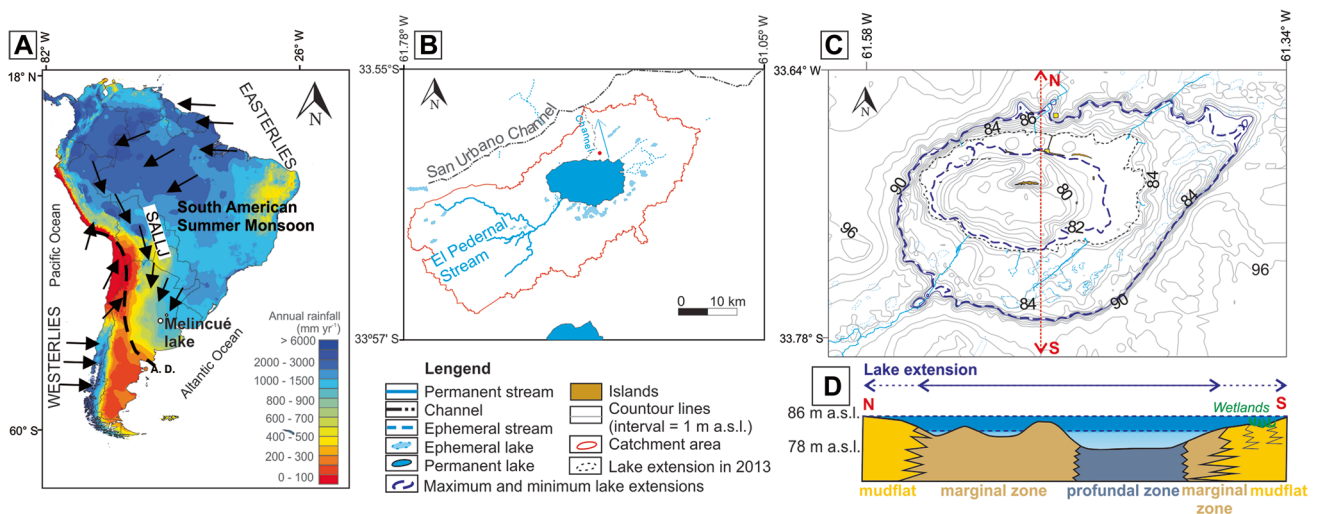


Fig. 1 Area setting of Lake Melincué. **a** South American annual rainfall (Hijmans et al. 2005) and climate features in South America. Arrows indicate the main wind direction of the South American Low Level Jets (SALLJ). The dashed line indicates the Arid Diagonal (AD) and the limit of the influence of the South American Summer Monsoon. The ellipse indicates the Pampean Plains location. **b** Lake Melincué watershed including channels, the red dot indicates the location of Melincué village. **c** Lake bathymetry and surrounding topography, modified from Guerra et al. (2015). Maximum and minimum lake extensions of this study are marked as blue dashed lines. Black short dashed line shows the year 2013 lake level when the bathymetry was measured. The N–S line (red) indicates the location of a profile from the northern to the southern shore. **d** N–S schematic profile showing the lake topography, the different subaquatic environments and lake water extension (modified from Guerra et al. 2015).

rain topography, modified from Guerra et al. (2015). Maximum and minimum lake extensions of this study are marked as blue dashed lines. Black short dashed line shows the year 2013 lake level when the bathymetry was measured. The N–S line (red) indicates the location of a profile from the northern to the southern shore. **d** N–S schematic profile showing the lake topography, the different subaquatic environments and lake water extension (modified from Guerra et al. 2015).

treaty about the conservation and wise use of wetlands and their resources; <https://rsis Ramsar.org/ris/1785>) and sustains large populations of vulnerable migratory waterbirds species such as the flamingo *P. andinus* (Romano et al. 2005, 2014). The humid Pampas further comprise the most important agricultural-livestock area of Argentina and these intensive productive activities prevail in the Melincué basin (Biasatti et al. 1999; Romano et al. 2014). In the northern shore of the lake, the village of Melincué is settled above the 85 m a.s.l. (Fig. 1b). During the years 1930s and 1960s a touristic expansion was promoted in the village and many of the infrastructure was built around the lake and on the islands formed by the topographic heights emerging during low lake-levels stages (Fig. 1c, d; Pasotti et al. 1984; Biasatti et al. 1999; Gatti 2010).

Recent analyses of hydrological data for the last four decades in SESA have shown significant positive hydrological balances (Barros et al. 2000; Compagnucci et al. 2002; Vera et al. 2006). They have increased river discharges and triggered unprecedented lake expansions causing floods with devastating impact in numerous shore villages and cities (Pasquini et al. 2006; Depetris 2007; Pasquini and Depetris 2010; Leroy et al. 2010; Córdoba et al. 2014). LM followed this trend, affecting the lakeshore infrastructures and part of the village, and negatively impacting on the former prosperous touristic industry. Floods of roads, rural areas and loss of connection with the islands were reported in 1966, 1973, 1974–1975, 1978, 2001 and 2003 (Pasotti et al. 1984; Table 1). As several parts of the village and nearby areas were inundated after the San Urbano channel was built in 1940 (Table 1; Fig. 1b), it was re-conditioned in 1977–1981 in order to prevent further floods. Additional works to protect the city area were done in 1985–1987 including a shielding embankment. During the 2003 high water stage LM expansion submerged the mudflats and advanced towards parts of the town (Fig. 1c, d). To prevent future flooding two pumping stations (able to extract $5 \text{ m}^3 \text{ s}^{-1}$) were built in 2005 to extract water from the lake during extreme high-stands and redirect it to the San Urbano Channel in order to maintain the lake level below an elevation of 82.5 m a.s.l. (Romano et al. 2014). In May 2017, however, the lake expanded again reaching its historical maximum extension and flooding the village.

2.2 Climate setting

The climate in the LM basin is subhumid to humid with an average annual precipitation for the region of 980 mm year^{-1} (1931–2011 period) and a mean annual temperature of $17.5 \text{ }^\circ\text{C}$ (1940–2013 period) (Pasotti et al. 1984; Guerra 2015; Guerra et al. 2015). Rainfall is strongly seasonal, with ca. 70% of the yearly precipitations falling during the austral summer. The rainfall variability in this area results from the interaction of different atmospheric circulation patterns with particular oscillation–frequencies (Zhou and Lau 2001; Garreaud et al. 2009). The main atmospheric feature supplying humidity from the Amazonian Basin and the Atlantic Ocean to South Eastern South America corresponds to the South American Monsoon (SAM, Zhou and Lau 1998; Vera et al. 2006) (Fig. 1a) that has seasonal variability. During the austral summer (from December to March), moisture is transported from the Atlantic Ocean and tropical Amazonia southward via a low level jet stream (South American Low Level Jet; SSLJ; Fig. 1a) through a low pressure belt formed between the Andes and the Brazilian Planalto. During the austral winter (from June to August), this humidity flux is deactivated and the precipitation in the Pampean Plains is reduced (Vera et al. 2006; Vuille et al. 2012).

In addition to this seasonal variability, precipitation in SESA is also controlled by atmospheric-oceanic phenomena occurring over the Atlantic and Pacific oceans with inter-annual and multi-decadal frequencies (Vera et al. 2006; Garreaud et al. 2009). Several authors have already pointed out the importance of Pacific modes regulating the SESA climate (e.g., Robertson and Mechoso 1998; Barros et al. 2008; Pasquini et al. 2006; Jacques-Coper and Garreaud 2015). El Niño–Southern Oscillation (ENSO) is considered as the most significant forcing of high-frequency climatic variability over most of South America (periodicity 2–7 years; Garreaud et al. 2009). Previous investigations have demonstrated the connections between El-Niño events with positive rainfall anomalies, increased river-discharges and lake-levels in the subtropical plains of the Paraná/La Plata River basin (Camilloni and Barros 2003; Pasquini and Depetris 2010). However, there is no uniform pattern along the Pampean Plains since major El Niño warm events only slightly correlate with well-documented lake-level oscillations in Lake

Table 1 Historical floods since 1965 (according to Pasotti et al. 1984; Biasatti et al. 1999; Peralta 2017)

Some of the reported floods (year)	Affected areas
1966	Touristic hotel in islands and coastal infrastructure, routes
1973	Roads
1974–1975	Touristic hotel in islands and coastal infrastructure, routes, rural population
2001	Overflow of the San Urbano channel
2003	Melincué village, routes

Mar Chiquita, located in the northern Pampean Plain (Troin et al. 2010, 2016). Low-frequency modes occurring in the Pacific Ocean, as the Pacific Decadal Oscillation (PDO, Mantua et al. 1997; Mantua and Hare 2002), and the Atlantic Ocean, as the Atlantic Multidecadal Oscillation (AMO, Enfield et al. 2001) have been suggested as an additional influence of South American rainfall regimes (Garreaud and Battisti 1999; Mantua and Hare 2002; Compagnucci et al. 2002; Chiessi et al. 2009; Krishnamurthy and Misra 2010). Furthermore, evidence of a connection between water depth, temperature and fish ecology with Pacific Ocean modes have been recently established in shallow Pampean lakes (Elisio et al. 2018).

3 Methodology

3.1 Lake water area variations from 1965 to 2015

A series of monthly lake-area oscillations was built using remote sensing data from 1972 to 2015. A total of 215 cloudless satellite images (Landsat 1–5 MSS 1972–1992; Landsat 5 TM 1984–2011; Landsat 7 ETM 1999–2014; Landsat 8 OLI_TIRS 2013–2015, U.S. Geological Survey; NASA) were acquired covering the last 40 years (1972–2015). Details of the remote sensing images used to derive lake areas are provided in Online Appendix 1. To determine the area of the lake (i.e., open water) on each image, we employed the image band with the highest available resolution (30 or 60 m). As the contrast between water and land pixels was high, the water area was automatically measured with the ImageJ software (Schneider et al. 2012). This software selects the pixels with the same value that the operator previously defined as water and counts the total number, delimiting the lake area. The pixel numbers occupied by lake waters were multiplied by the pixel area (900 m² or 3600 m²) to quantify the lake area. At least two images of every year were measured and when more than one image was available for a month, they were averaged to obtain a single monthly value.

Additional data of LM water fluctuation are provided by lake level data from multiple sources, including publications (Pasotti et al. 1984; Romano et al. 2005), local reports (Biasatti et al. 1999; Peralta 2003; Romano et al. 2014), a MSc thesis (Palamedi 2006) and personal communications from the local population. To enlarge our monthly dataset of lake area fluctuations obtained through the satellite images ($n = 209$; excluding repeated areas within the same month), we merged this data with the available monthly lake-level data since 1965 ($n = 200$). Both records overlap 64 months. We preferred to base our reconstruction on the satellite-derived lake

area over the lake level because of two main reasons. Firstly, the lake area data we used was obtained from a unique and accessible source (i.e., Landsat images) following a straightforward methodology. In contrast, the LM lake-levels were randomly measured by different observers. In addition, the flat landscape of the Pampean Plains implies that small lake level variations represent large areal changes, which are easily observed through the satellite images. Because of both reasons, i.e., the uniformity of the sources and the amplified signal provided by lake areas, we considered these data as the best record of the lake fluctuations.

A linear regression equation ($y = ax + b$) was obtained with the values corresponding to 64 overlapping months of the lake area (y) and lake level (x) data. The regression significance was evaluated through the R^2 coefficient and compared with a hypsometric curve of the lake topography, which was constructed from a ASTER Global Digital Elevation Model (GDEM) of ~30 m resolution. The linear regression allowed us to calculate the lake area of those months when only the lake level was available ($n = 136$). Therefore, a total of 345 monthly lake areas were reconstructed using both methodologies (i.e. Landsat satellite images and linear regression of lake level).

Using the discrete monthly lake areas, we constructed an annual and seasonal lake area series from 1965 to 2015. The annual lake area was calculated as an average of the available months during the precipitation cycle in the region of interest (July–June). Seasonal lake areas included the dry semester (April–September) and the humid semester (October–March). In order to compare the significance of the intrannual with the inter-annual variability of lake area oscillation, we calculated the coefficients of variation (CV) for both data (e.g. Morales et al. 2015). An autocorrelation test was applied as well on every series to identify the persistence of the lake monthly and annual variations over the period 1965–2015.

In order to compare the lake area variation to different hydrological and climatic parameters, we standardized this variable (Hipel and McLeod 1994). We assumed the lake watershed reduction (occurred in 1930s) and the intermittent pumping of water from the lake (starting in 2005) as the main anthropogenic lake modifications that may have influenced the lake area dynamics. Therefore, the seasonal and annual total series (1965–2015) were standardized for the period 1965–2004, i.e. previous to the activation of the pumping activities, as follows:

$$LA_{t1} = (la_{t1} - \text{mean } la) / (sd) \quad (1)$$

where LA_{t1} is the standardized lake area of the year $t1$, la_{t1} represents the lake area of the year $t1$, and the *mean la* and *sd* are the average and the standard deviation of the period 1965–2004.

3.2 Climate data

Gridded precipitation and temperature data for the period 1965–2015 was obtained from CRU data $0.5^\circ \times 0.5^\circ$ cell series (Harris et al. 2014) centered at LM ($33^\circ\text{S}/61.25^\circ\text{W}$). The location of the different stations is detailed in Table 2.

A standardized precipitation–evapotranspiration index (SPEI; Vicente-Serrano et al. 2010) for the period 1965–2015, also centered at LM, was obtained from the monthly gridded data of the Global SPEI database (<http://sac.csic.es/spei/database.html>). This index is based on a water balance equation (precipitation–potential evapotranspiration) and in its formulation also includes the evaporative demand (caused by temperature fluctuations), in the present context of global warming, indicating wet, dry and normal years in a region (Vicente-Serrano et al. 2010; Beguería et al. 2014).

All of the analyzed climatic series were annually averaged (according to the July–June hydrological year) and standardized with respect to the period 1965–2004 by using the same methodology of Eq. (1) for each case.

In order to compare the local record (i.e., lake area) with large-scale climate indices, we obtained monthly data of

El Niño 3.4 (<https://www.esrl.noaa.gov/psd/data/correlation/nina34.data>), PDO (<https://www.esrl.noaa.gov/psd/data/correlation/pdo.data>), and the Atlantic Multidecadal Oscillation index (AMO; <https://www.esrl.noaa.gov/psd/data/correlation/amon.us.data>; Enfield et al. 2001).

The obtained results included annual standardized anomalies for the period 1965–2015 of precipitation (SPA), temperature (STA) and SPEI, as well as El Niño 3.4 and PDO and AMO indices.

3.3 Frequencies and correlation with global climate indices

Spectral estimates including Lomb's Periodogram and a Continuous Wavelet Transform (Torrence and Compo 1999) were performed over the standardized annual lake areas (LA July–June) to detect the dominant low frequency modes and to localize them in time. For wavelet analysis, the Morlet wavelet was used to better understand the time–frequency field. The wavelet analysis was applied on detrended series by subtracting a linear fit from the annual data.

Pearson correlation was applied on the dataset to distinguish the main hydrological relationships among all

Table 2 CRU TS 3.23 station list used in the gridded temperature and precipitation data

Station list				
CRU TS 3.23 station	Station ID	Latitude	Longitude	Temporal cover
Temperature				
Pilar Observat	8734900	31.67S	63.88W	1931–2015 current
Rafaela/INTA	8735900	31.20S	61.60W	1961–1992
Sauce Viejo AI	8737100	31.70S	60.82W	1961–2000
Parana Aero	8737400	31.78S	60.48W	1876–2015 current
Marcos Juarez	8746700	32.70S	62.15W	1961–2015 current
Rosario Aero	8748000	32.92S	60.78W	1941–2015 current
Guauguaychu A	8749700	33.00S	58.62W	1961–2015 current
Laboulaye Aero	8753400	34.13S	63.37W	1961–2015 current
Pergamino/INTA	8748400	33.90S	60.60W	1912–1993
Junin Aero	8754800	34.55S	60.92W	1933–2015 current
General Pico A	8753200	35.70S	63.75W	1952–2015 current
Pehuajo Aero	8754400	35.87S	61.90W	1951–2015 current
Nueve de Julio	8755000	35.45S	60.88W	1907–2010
San Miguel	8756900	34.55S	58.73W	1933–1993
General Pico A	8753200	35.70S	63.75W	1952–2015 current
Precipitation				
Marcos Juarez	8746700	32.70S	62.15W	1898–2015 current
Rosario Aero	8748000	32.92S	60.78W	1875–2015 current
Junin Aero	8754800	34.55S	60.92W	1896–2015 current
Casilda	8747400	33.04S	61.17W	1901–1988
Parana Aero	8737400	31.78S	60.48W	1875–2015 current
Nueve de Julio	8755000	35.50S	60.90W	1897–2010
General Pico A	8753200	35.70S	63.75W	1907–2015 current
Villaguay	8738500	31.85S	59.08W	1900–1990

analyzed variables, including the standardized annual Lake Area, SPA, STA and SPEI (regional), and annual El Niño 3.4, and PDO indices (large-scale). In order to explain possible lags in the lake area response to climate drivers, the standardized SPA and SPEI were filtered using a direct band-pass filter of 20 years to cross correlate them with the standardized annual lake area.

4 Results

4.1 Temporal changes of lake surface area

The reconstructed monthly lake area series for the period 1965–2015 summed a total of 345 data points and 267 missing months (see supplementary data). The mean difference between measured monthly areas (satellite) and calculated monthly areas from the lake level is 3.20 km², corresponding to 3.4% of the mean measured area (Fig. 2a, b). The mean monthly lake area is 94.52 km² and the standard deviation is 24.57 km² (Fig. 2c). Maximum and minimum lake water extensions were 147.44 km² in August 2003 and 42.47 km² in February and March 1966, respectively (Fig. 2c; Table 3). In seasonal cycles, the maximum lake extensions are reached during the autumn and winter seasons (i.e., the dry season in the Pampean Plains), while minimum extensions distribute along the summer months (i.e., during the rainy and warm season) and the month of September (Fig. 2d).

In average, the mean intra-annual variation is 20 km² (Fig. 2c), while inter-annual oscillations show larger amplitudes (Fig. 2c; Table 3). The morphometric data for the

1965–2015 period indicate that the surface fluctuated Δ 90.7 km² and the water level oscillated Δ 3.5 m (Fig. 2a, b). Nevertheless, estimations for the beginning of the century suggest that the surface variation was even larger. Castellanos (1924) described the lake as separated in two minor water bodies, which points to shallower and contracted lake conditions (that would correspond to a depth < 2.5 m and an area around 22 km²), according to the bathymetric data.

The calculated annual (LA Jul–Jun) and seasonal lake areas (LA Oct–Mar and LA Apr–Sep) show similar variability and mean values, standard deviations (SD), and coefficients of variation (CV) and autocorrelation (Table 3). Due to the similarities between these three indices, we selected the annual series (LA Jul–Jun) as representative to describe the inter-annual lake area variability to compare it with the rest of the climatic variables. The CV calculated for the inter-annual variability series is an order of magnitude larger (~24–25) than the intra-annual variability (~3) (Table 3). The autocorrelation results show consistent 2-year significant persistence of the annual (lag = 1–2 years) and monthly (lag = 18 months) series (Table 3).

In general, reduced lake areas occurred before 1975, the intervals 1985–1990 and 2008–2013, while considerable expansion phases were reached during the periods 1975–1985, 1990–1997 and 2000–2007 (Fig. 2d).

The Lomb's periodogram of lake annual area (LA Jul–Jun) series indicates a significant period corresponding to ~20 years (frequency = 0.05; Fig. 3a). This periodogram shows a secondary noticeable peak around the 13 years period (frequency = 0.075) although it is non-statistically significant.

Table 3 Basic statistics and autoregressive results for the different reconstructed lake areas (LA): mean monthly, annual (Jun–Jul), wet season (Oct–Mar); dry season (Apr–Sep); and the temperature, precipitation, their standardized anomalies (STA and SPA) and the standardized SPEI

	Inter-annual variability	Intra-annual variability			Temperature/STA	Precipitation/SPA	SPEI Jul–Jun
	LA-monthly	LA Jul–Jun	LA Oct–Mar	LA Apr–Sep	Jul–Jun	Jul–Jun	
Basic statistics							
Period	1965–2015	1965–2015	1965–2015	1965–2015	1965–2015	1965–2014	1965–2015
N	345	50	49	50	50	49	50
Missing data	267	0	1	0	0	1	0
Min	42.47	56.92	49.93	56.25	14.91**	601.4**	– 0.71
Max	147.43	138.96	138.28	143.76	17.71**	1366.6**	0.74
Mean	94.52	93.62	95.45	98.18	16.79**	957.41**	0.11
SD	3.38*	23.96	23.84	23.93	0.41	175.82**	0.31
CV	3.42*	25.59	24.98	24.38	2.43	2315.57	288.82
Autocorrelation							
Lag (significant)	18 (max)	2 (max)	2 (max)	2 (max)			
Autocorrelation coefficient	>0.49	>0.71	>0.65	>0.69			
p value	<0.05	<0.01	<0.01	<0.0025	Non-significant	Non-significant	Non-significant

*Calculated on the mean monthly areas; **Correspond to the Jul–Jun series without standardization

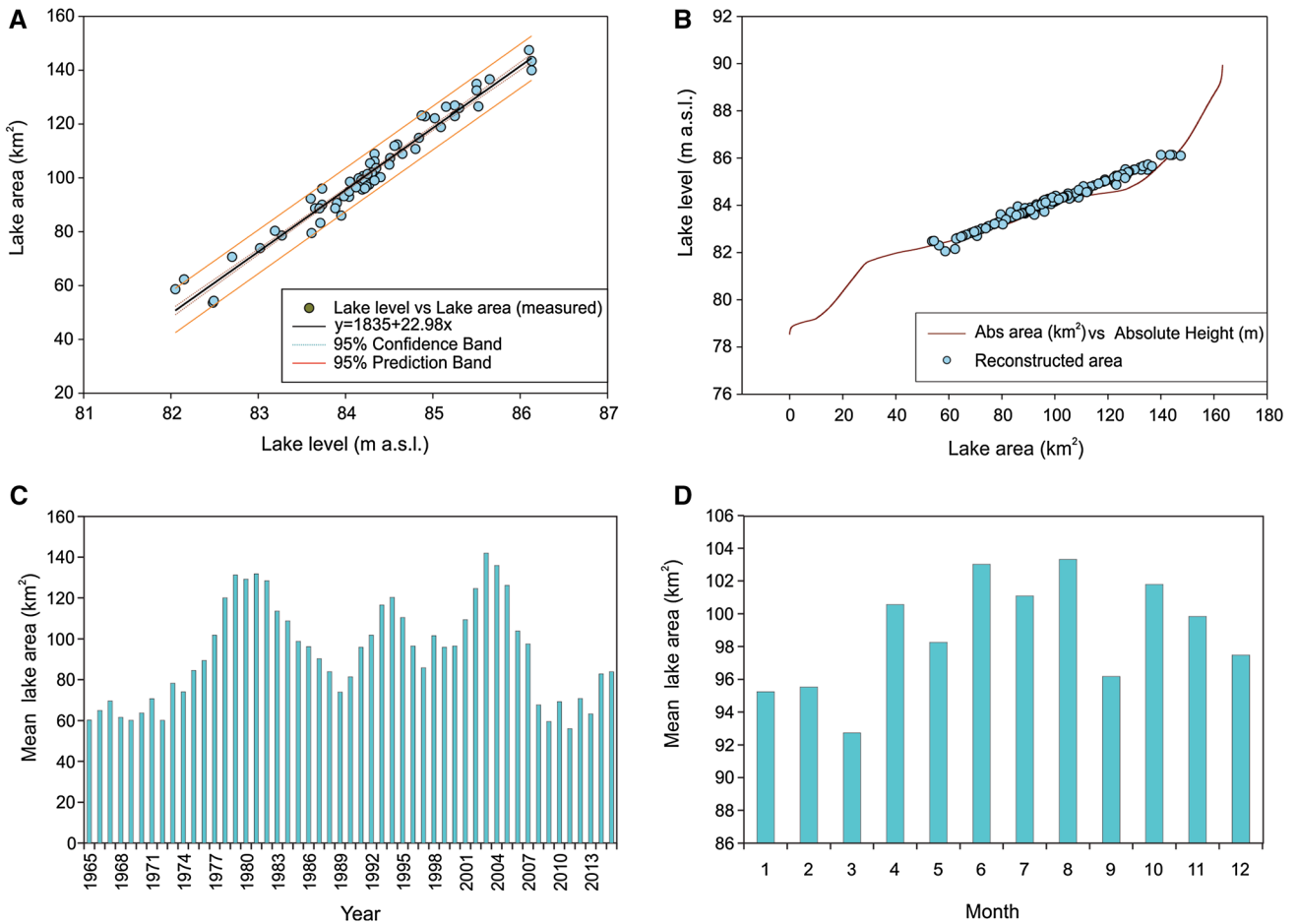


Fig. 2 Reconstruction of the Lake Melincué area for the period 1965–2015. **a** Linear regression curve of the in situ measurements of monthly lake water levels vs. lake areas measured from satellite images for the same years. **b** Reconstructed area (blue dots) for the period 1965–2015, including the measured area from satellite

data and the calculated area from lake levels through the equation $y = 1835 + 22.98x$; and lake hypsometry (curve). **c** Annual lake area fluctuation for the period 1965–2015. **d** Mean monthly lake area (period 1965–2004)

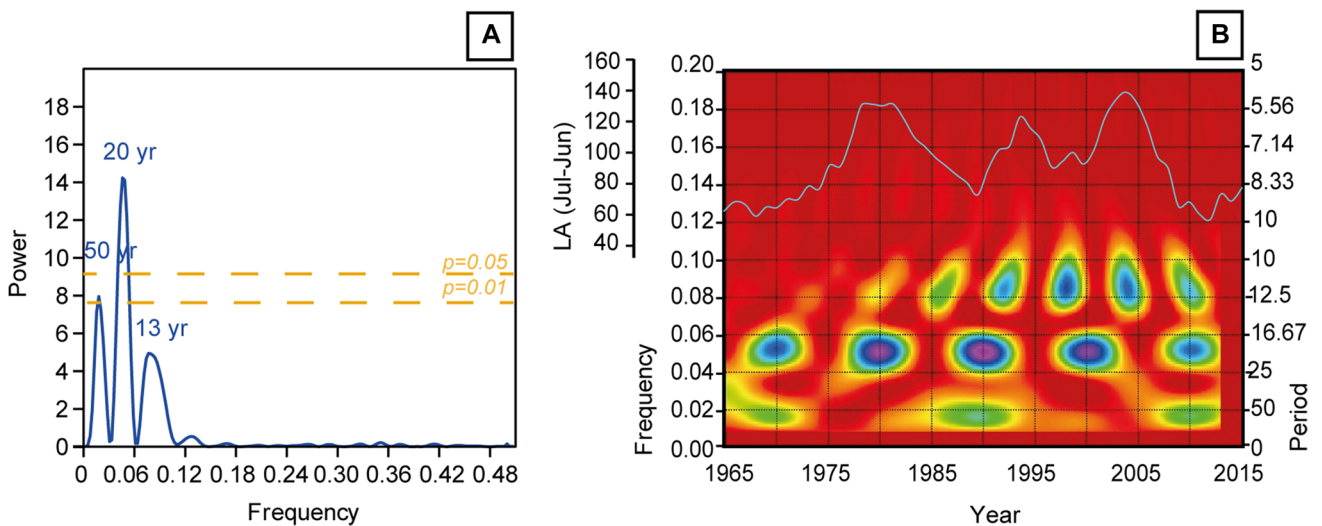


Fig. 3 Spectrum analyses of the annual lake area (LA Jul–Jun). **a** Periodogram. Yellow discontinuous lines correspond to $p=0.05$ and $p=0.01$. **b** Wavelet analysis in the frequency spectrum and the annual lake area (LA Jul–Jun, km^2)

Fig. 4 Climate time series. **a** Annual, seasonal and monthly lake areas (LA Jul–Jun; LA Oct–Mar; LA Apr–Sep; monthly LA). The shadowed yellow area indicates the period with pumping operations in the lake. **b** Standardized precipitation anomaly (SPA) and 20 year filtered SPA (NOAA). **c** Standardized evaporation-precipitation index (SPEI) and 20 year filtered SPEI (Vicente-Serrano et al. 2010). **d** Standardized temperature anomalies (STA) and 20 year filtered STA (NOAA). **e** Annual Pacific Decadal Oscillation (PDO) from NOAA, and 20 year filtered PDO. **f** Annual El Niño 3.4 index and 20 year filtered (NOAA). Stars indicate “very strong” El Niño events. **g** Atlantic Oscillation Mode (AMO) and 20 year filtered AMO. Blue columns indicate periods of lake expansion. Dashed lines mark the mean and the standard deviation values of each parameter

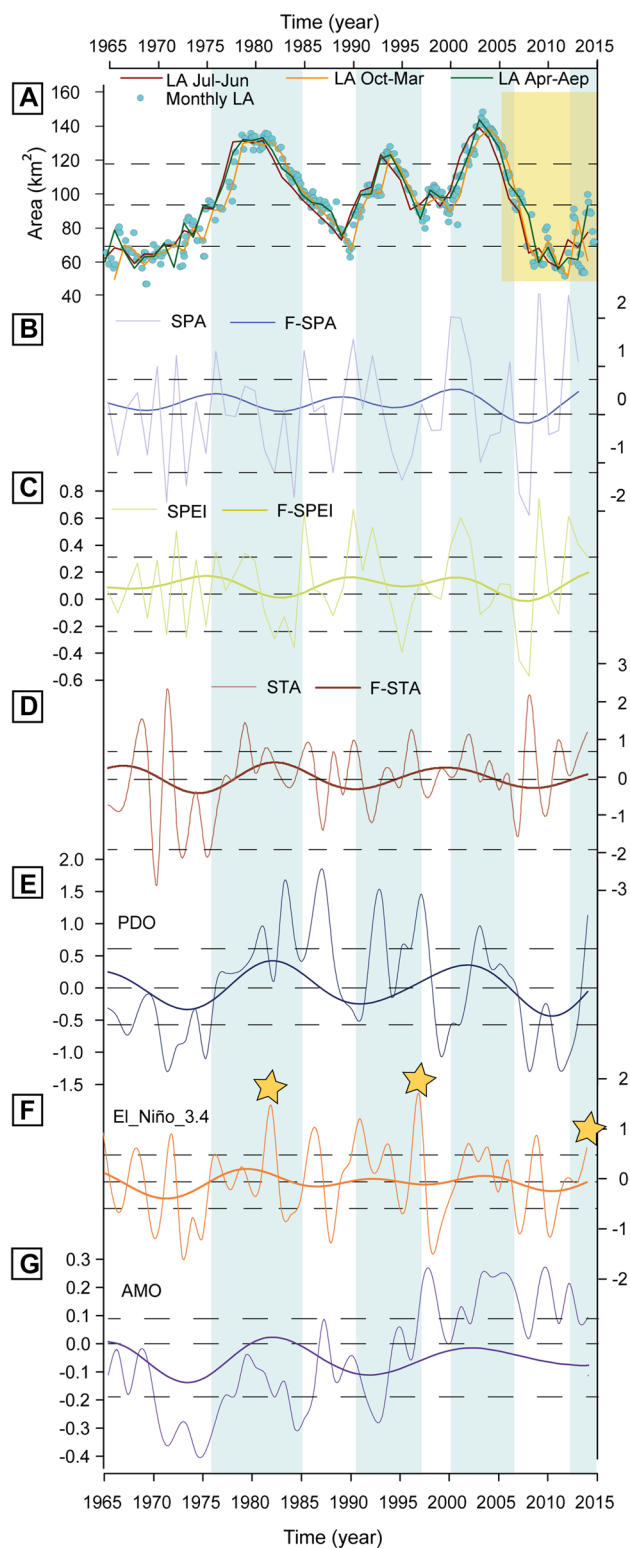
The wavelet analysis in annual areas time series captured lower-frequency variations and supplied further findings about the time domain of the main periods. The power spectrum showed significant oscillations with a period of about 20 years (17–25) along the time series, with higher intensities during the intervals 1964–1967; 1978–1983; 1987–1993; 1996–2004; 2006–2015 (Fig. 3b). A period quasi-decadal of ~12.5–13 years starting in 1977 was also observed along the record, coincident with a substantial increase in lake area.

4.2 Climatic fluctuations and the relationship with the LM area

The basic statistics of the regional meteorological variables and the calculated standardized indices are summarized in Table 3. Lake Melincué area (LA), standardized anomalies of the temperature (STA), precipitation (SPA), SPEI index are shown in Fig. 4a–d). The large-scale oceanic indices variations are represented in the Fig. 4e–g.

During the period of 1965–2015, the mean temperature and precipitation of LM basin were 16.79 °C and 957.41 mm, respectively. The overall SPA and SPEI behavior showed similar inter-annual variability without a significant trend. Nevertheless, during the analyzed period of the record the wet peaks have incremented their amplitudes (Fig. 4b, c). The temperature index, on the other hand, shows relatively smaller negative excursions after 1975 (Fig. 4d).

The Pearson correlation coefficients show that the lake annual area is not significantly correlated with the SPA, SPEI, or the STA (Table 4). Figures 4 and 5 allow visualizing that the lake area and climate variations are not exactly in phase. Contrastingly, the cross-correlation coefficients indicate that the highest correlation is reached with a 20 years filtered-SPA ($r=0.82$; Fig. 5a) with a lag of 3 years and with a 20 years filtered-SPEI ($r=0.75$), with a lag of 4 years (Fig. 5b).



When the lake areas are compared with the global climatic oscillation modes, the Pearson coefficient indicate the most significant positive correlation with the PDO and a positive correlation with El Niño 3.4 index (Table 4).

Table 4 Correlation matrix between the analyzed variables and the annual lake areas (LA, Pearson coefficient/p)

Pearson correlation	STA	SPA	LA	SPEI	El-Niño 3.4	PDO	AMO
STA	0	0.50	0.41	0.97	0.06	0.93	0.25
SPA	-0.10	0	0.82	8.68E-24	0.02	0.64	0.33
LA-Jul-Jun	0.11	-0.03	0	0.93	0.14	1.56E-4	0.51
SPEI	-0.01	0.94	0.01	0	0.02	0.83	0.67
El-Niño 3.4	0.25	0.322	0.21	0.32	0	0.03	0.26
PDO	-0.01	-0.06	0.50	-0.02	0.29	0	0.55918
AMO	0.16	0.14	0.09	0.06	0.16	0.08	0

Bolded numbers indicate significant correlations with the LA

5 Discussion

5.1 Hydro-climate variability and connections across the period 1965–2015

A discussion of the Pampean Plains' lake area changes, their frequency and causes should be addressed from different angles considering a multiple time and space-scale approach. In particular, regional rainfall associated with the

dynamics of the SAM is characterized by a marked temporal variability and controls the hydrological balance of the LM (Guerra et al. 2015, 2017). Our current results have shown that within the intra-annual signal, the LM area generally increases during the dry season and reduces during the rainy season. This signal indicates that a factor different than rainfall contributed to the intra-annual lake area variability, which can be attributed to evaporation and/or infiltration processes acting seasonally on this system. A similar behavior, i.e. higher monthly lake levels during winter and lower in summer, was detected in the closed-lake Mar Chiquita, located in the Pampean Plains at 30° SL (Troin et al. 2010), which have been linked to the seasonal evaporation regime (low in winter and high in summer). Comparable mechanisms could be affecting the intra-annual variability in the LM area. In contrast, on inter-annual scales our reconstruction of the annual lake area indicated that the expansions are led by rainy years. Although both results (intra- and inter-annual) may seem contradictory, the variation (CV) and autocorrelation coefficients allow demonstrating that the inter-annual lake-area variability prevails over the intra-annual variability.

Although rainfall is the obvious driver of the Pampean lakes' water fluctuation, our results show that there is a lack of synchronicity of LM-area series with the SPA and SPEI as shown by low Pearson correlation coefficients. The cause of this asynchronous behavior is a 3–4 years lag between the beginning of the lake expansion and the increases in rainfall (Fig. 5). This could be related to buffer effects produced by one or more interacting hydrological processes including either, a delay caused by processes of infiltration, smaller temporary wet meadows retarding inflow into the lake, evapo-transpiration and/or previous soil wetness and lakestand conditions. Evidence of larger lag values found in the filtered SPEI (4 years) compared to the lag of the filtered SPA (3 years), suggests that outflow by evaporation is a slower process than inflow by precipitation. Comparable results have been reported in previous studies that have documented lags from 6 to 24 months between changes in precipitation and levels of groundwater and reservoirs (Vicente-Serrano et al. 2010; Díaz et al. 2013). However,

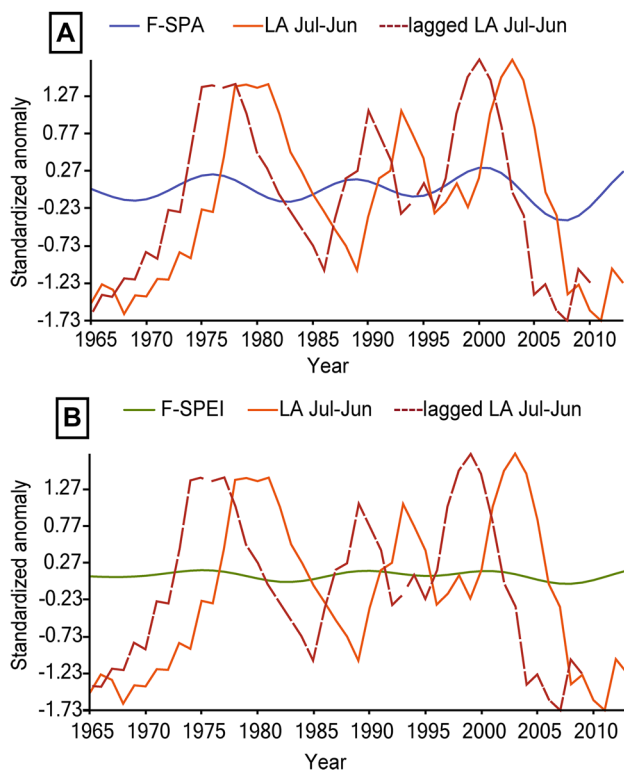


Fig. 5 Lags of the Melincué annual lake area corresponding to the cross-correlation results. **a** Lag=3 years detected between the 20-year filtered Jul–Jun SPA (standardized precipitation anomalies) and the lake area (LA). **b** Lag=4 years detected between the 20-year filtered Jul–Jun SPEI (standardized precipitation–evaporation index) and the lake area (LA)

the lack of statistically significant correlation between areal changes and temperature suggest a negligible effect of local temperature modulating changes in LM dynamic.

A closer focus into the monthly and annual lake series shows that the initial lake condition is a crucial factor for the sign and magnitude of the following lake area fluctuations. Thus, if an initial condition of expanded lake area is followed by a short dry period, the lake area will be maintained and continue its expansion only after the next rainy season. For instance, Fig. 6 shows an insight of the monthly lake area and the precipitation from 2001 to 2005. After the raising rainfall occurred in April 2001, the lake immediately expanded. Dry conditions prevailed in May 2001 but instead of contracting the lake maintained a similar area. In August of the same year the lake area increased more than in the previous wet period, even though both intervals had similar average rainfall. The subsequent period from 2002 until 2004 presented a general decrease in precipitations. Nevertheless, the monthly lake area record shows frequent phases of stability and expansion with only a few negative peaks. Thus, after a period of frequent positive precipitation anomalies, the time needed for outflow by evaporation is longer than the time for lake expansion by inflow.

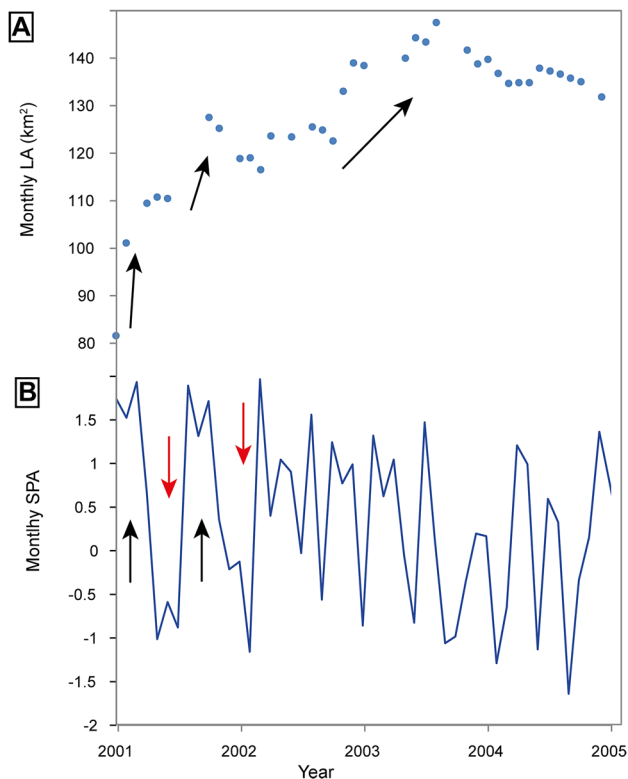


Fig. 6 **a** Monthly lake area (LA-monthly, km²) and **b** standardized precipitation anomalies (SPA) between 2001 and 2005. Arrows exemplifies months and phases of increasing (black) and decreasing (red) values of the analyzed variables

The resilient behavior of the lake areas may explain the long term inter-annual variability of the series. Furthermore, the spectral analysis shows that the annual lake area record was not characterized by high-frequency (i.e., < 10 years) inter-annual oscillations. Besides, although there is a positive correlation between the lake area and El Niño 3.4 index, which is characterized by 5–7 year signals, the “very strong” El Niño warm and rainy events of 1982–1983 and 1997–1998 were not immediately followed by an increase in lake area (Fig. 4). These findings agree with previous studies in streamflows and lake level series from central Argentina, where the high frequency ENSO signal is hard to discern (Penalba and Vargas 2004; Pasquini et al. 2006; Troin et al. 2016). This seasonal dependence is probably reflected as a weak teleconnection influencing the LM. Thus, the analysis of ENSO impact appears to be not significant at scales of year-to-year variability although at decadal to multi-decadal scales the association could become relevant (Andreoli and Kayano 2005; Barreiro 2010).

The main pattern found in the analysis of LM area is quasi-bidecadal in the band of 17–25 years, extending from the beginning of the record (1965) to present-day (2015), as pointed by the spectral and wavelet analyses. This lower frequency band is in accordance with a significant 16–21 years periodicity recognized in spectra of global SSTs of Southern Hemisphere oceans by Folland et al. (1999). Likewise, the periodicities are also in agreement with those found by Compagnucci et al. (2002) in central-western Argentina.

Additionally, the spectral results point to a quasi-decadal periodicity around 13 years in the annual lake area that had an onset just after the mid-1970s (Fig. 3), which is consistent with the long and persistent wet spell recorded from 1973 up to the beginning of the twenty-first century across SESA (Compagnucci and Agosta 2008; Seager et al. 2010; Russián et al. 2015). Thus, the lake areas showed a relevant change in the low-frequency variability during this period. Several unprecedented highstands were registered by 1970s in the instrumental and sedimentological Pampean lake records (Piovano et al. 2002; Córdoba et al. 2014, 2017; Guerra et al. 2015, 2017). Moreover, this extended humid period represents the longest prolonged wet spell of the last centuries in this part of South America (Compagnucci et al. 2002; Piovano et al. 2009; Agosta and Compagnucci 2012). It has been linked to a positive precipitation jump occurred in SESA (Berbery and Barros 2002; Agosta and Compagnucci 2008; Jacques-Coper and Garreaud 2015), associated with the 1976–1977 cold to warm change in tropical sea surface temperatures of the Pacific Ocean (e.g., Miller et al. 1994; Giese et al. 2002; Huang et al. 2005; Jacques-Coper and Garreaud 2015). The latter has been in turn related to a change in phase of the PDO index, separating a ‘La Niña-like’ decadal regime from an ‘El Niño-like’ one (Garreaud

et al. 2009; Meehl et al. 2013; Newman et al. 2016). The lake-area record also shows a high significant correlation with the PDO index that is in agreement with these patterns. The consistency LM-PDO variability may confirm the large-scale climatic influence on the oscillation of local lake areas dynamics in this part of South America.

Our results demonstrate that the standardized LM-LA and the AMO do not correlate, although an Atlantic influence in hydrological dynamics of Pampean lakes cannot be discarded. Other investigations have examined the effect of variability on SESA precipitation, identifying links to sea surface temperature anomalies in the subtropical and tropical Atlantic Ocean (Nogués-Paegle et al. 2002; Paegle and Mo 2002; De Almeida et al. 2007; Taschetto and Wainer 2008; Seager et al. 2010). Likewise, recent studies showed that a wet trend from the mid-1970 to the early 2000s has been largely forced by a relative cooling of the tropical Atlantic Ocean that is related to the cool phase of the AMO (Folland et al. 1999; Seager et al. 2010). The AMO appears to be shifting toward its positive phase following this cooling (Ting et al. 2009; Seager et al. 2010), which forces a decrease in SESA precipitation in the subsequent years and decades. The AMO has as well been linked to changes in the ENSO and PDO, which interaction regulates the South American climate (d'Orgeville and Peltier 2007; Kayano and Capistrano 2014). Thus, the multi-decadal Atlantic SST influence on precipitation in the Pampean Plains and in the LM dynamics should be addressed with further detail.

5.2 Anthropogenic influence vs. natural variability

A still open question is whether changes in lake areas have or have not been conditioned by anthropogenic modifications of the watershed, and the quantification of this on their variability. Historical documents indicate that the Melincué village developed during lowstand periods (Peralta 2017) and, consequently civil infrastructure was designed for reduced lake areas. Interestingly, water-regulation works have been projected as consequence of the overflows, but they started functioning subsequently, coinciding with the following dry cycles. For instance, in the 1930s the LM shores were swamped but the San Urbano channel that was planned to solve this problem was only finished after 1942, coinciding with a low precipitation regime that extended until the 1950s (Romano et al. 2014). Analogously, the pumping that was planned as a reaction to previous floodings, started functioning in 2005, partially coinciding with a dry period and major lake contractions across the Pampean Plains by 2008–2009. As the management of lake water accompanies naturally-induced hydrological changes, the human impact in the lake catchment is not easily distinguished from climatic triggers. In many occasions, the management works in the Pampean lakes have not been efficient enough to solve the flooding

problems (Leroy et al. 2010; Peralta 2017), and their implementation during the low-water stages, when water volume regulation is not needed, trigger uncertain ecological changes of the lake (Romano et al. 2014). Further detailed studies quantifying the human-induced changes (e.g. land use changes) would be useful to discern the anthropogenic contribution to the lake intra- and inter-annual variability and its consequences on the lake system.

Our findings have important implications for both, the interpretation of past lake area records and the forecast of future responses of Pampean lakes to climate change. Here we suggest that the observed trend and variability of the LM areas is strongly influenced by natural multi-decadal oscillations of the climate system. However, it is not possible to differentiate if the 1976–1977 increment of periodicity of the lake area could be linked to anthropogenic global warming (Trenberth 1990) or to natural forcings (Seager et al. 2010). Recently, Meehl et al. (2009) interpreted this shift as a consequence of changes in external forcing, particularly the increase in atmospheric greenhouse gases, superimposed upon inherent decadal fluctuations of the Pacific Ocean (Jacques-Coper and Garreaud 2015). Although hydroclimatic simulations and models of SESA have predicted increasing rainfall for the next years under a climate warming trend (Chou et al. 2013; IPCC 2014), the analysis of our data shows that LM area was not linearly responsive to temperature changes in recent years (IPCC 2014). Thus, improving our understanding of the causes behind inter-annual to multidecadal precipitation variability in the region and the response of LM has important implications for interpreting past records of lake areas and for anticipating lake hydrological variations in the context of future climate change. Forecasting the lake area variability in the coming decades is crucial for infrastructure planning and the sustainable development of this important and productive region of South America.

6 Conclusions

This study provides a database of the LM area changes from 1965 to 2015 based on reliable and accessible information provided by satellite imagery. Our results show that LM has been very sensitive to changes in the regional climate over this 50 years interval. The lake area variability of this Pampean lake has been determined at different frequencies and considered within a regional and large-scale climate dynamics. Among the analyzed climatic variables, the most important drivers of the annual lake area changes are precipitation and evaporation, although both inducing different time-responses. The variability of the monthly and annual lake area shows that inter-annual oscillations predominate over intra-annual variations. The spectra show a prevailing

low frequency signal, mainly quasi-bidecadal (17–25 years), throughout the studied period. A secondary 13 years signal was detected after 1970s, which pointed to more frequent expansion–contraction cycles occurring since that decade. At a larger scale there is a good correlation between lake area changes and Pacific ocean–atmosphere modes, confirming the connection between large-scale climate forcings and local lake water changes.

The behavior of this lake is comparable to most of the shallow lakes in the Pampean Plains region. Thus, our results point toward an urgent need to further monitor the Pampean lakes' water areas focusing in the low frequency variability in order to plan effective water management strategies. Understanding how Pampean lakes respond to a variable climate will allow a better managing of local water resources as well as the protection of areas under flood risk. Furthermore, determining the tempo and pace of these lake area changes is crucial for the development of novel strategies to cope with future climatic scenarios and, thus, of major societal interest.

Acknowledgements Part of the results of this investigation have been carried out at CICTERRA (CONICET/Universidad de Córdoba, Argentina). This study was funded by the FONCyT (PICT 2013-1371). Most of the manuscript was written at the Department of Earth Sciences, University of Geneva, Switzerland under a Swiss Government Excellence Scholarship (2017–2018). We sincerely thank the editor and the reviewers for their comments and helpful suggestions. We also thank Marcelo Romano, from the *Centro de Investigaciones en Biodiversidad y Ambiente, Rosario*, who shared lake level data and Don Raúl Rébora from Melincué.

References

- Achaga RV, Irurzun MA, Gogorza CSG et al (2017) Paleomagnetic and paleoclimatic investigation at Laguna Melincue (Pampean Plains, Argentina): preliminary results. *Stud Geophys Geod* 61:318–335. <https://doi.org/10.1007/s11200-016-1247-0>
- Agosta EA, Compagnucci RH (2008) The 1976/77 austral summer climate transition effects on the atmospheric circulation and climate in Southern South America. *J Clim* 21:4365–4383. <https://doi.org/10.1175/2008JCLI2137.1>
- Andreoli RV, Kayano MT (2005) ENSO-related rainfall anomalies in South America and associated circulation features during warm and cold Pacific decadal oscillation regimes. *Int J Climatol* 25(15):2017–2030
- Barreiro M (2010) Influence of ENSO and the South Atlantic Ocean on climate predictability over Southeastern South America. *Clim Dyn* 35:1493–1508. <https://doi.org/10.1007/s00382-009-0666-9>
- Barros V, González M, Liebmann B, Camilloni I (2000) Influence of the South Atlantic convergence zone and South Atlantic sea surface temperatura on interannual summer rainfall variability in Southeastern South America. *Theor Appl Climatol* 67:123–133
- Barros V, Doyle M, González M, Camilloni I, Bejarán R, Caffera RM (2002) Climate variability over subtropical South America and the South American monsoon: a review. *Meteorologica* 27(1–2):33–57
- Barros VR, Doyle ME, Camilloni IA (2008) Precipitation trends in southeastern South America: relationship with ENSO phases and with low-level circulation. *Theor Appl Climatol* 93(1–2):19–33
- Beguiería S, Vicente-Serrano SM, Reig F, Latorre B (2014) Standardized precipitation evapotranspiration index (SPEI) revisited: parameter fitting, evapotranspiration models, tools, datasets and drought monitoring. *Int J Climatol* 34(10):3001–3023
- Berbery EH, Barros VR (2002) The hydrologic cycle of the la Plata basin in South America. *J Hydrometeorol* 3:630–645. [https://doi.org/10.1175/1525-7541\(2002\)003%3C0630:THCOTL%3E2.0.CO;2](https://doi.org/10.1175/1525-7541(2002)003%3C0630:THCOTL%3E2.0.CO;2)
- Bianchi LO, Rivera JA, Rojas F et al (2017) A regional water balance indicator inferred from satellite images of an Andean endorheic basin in central-western Argentina. *Hydrol Sci J* 62:533–545. <https://doi.org/10.1080/02626667.2016.1247210>
- Biasatti N, Delannoy L, Peralta E, Pire E, Romano M, Torres G (1999) Cuenca Hidrográfica del Humedal de la Laguna Melincué, Provincia de Santa Fe. ProDIA, SRNyDS, Buenos Aires
- Bohn VY, Delgado AL, Piccolo MC, Perillo GME (2016) Assessment of climate variability and land use effect on shallow lakes in temperate plains of Argentina. *Environ Earth Sci* 75:1–15. <https://doi.org/10.1007/s12665-016-5569-6>
- Camilloni IA, Barros VR (2003) Extreme discharge events in the Paraná River and their climate forcing. *J Hydrol* 278(1):94–106
- Castellanos A (1924) Contribución al Estudio de la Paleoantropología Argentina. Restos Descubiertos en el Arroyo Cululú (Pcia. de Santa Fe). *Revista de la Universidad Nacional de Córdoba* 11:7–9
- Chiessi CM, Mulitza S, Pätzold J et al (2009) Possible impact of the Atlantic multidecadal oscillation on the South American summer monsoon. *Geophys Res Lett* 36:1–5. <https://doi.org/10.1029/2009GL039914>
- Chou C, Chiang JCH, Lan CW et al (2013) Increase in the range between wet and dry season precipitation. *Nat Geosci* 6:263–267. <https://doi.org/10.1038/ngeo1744>
- Compagnucci R, Agosta E (2008) La precipitación de verano en el centro-oeste de Argentina y los fenómenos interanual el niño/oscilación sur (ENOS) e interdecadal “tipo” ENOS. *Geoacta* 33:107–114
- Compagnucci RH, Agosta EA, Vargas MW (2002) Climatic change and quasi-oscillations in central-west Argentina summer precipitation: main features and coherent behaviour with southern African region. *Clim Dyn* 18:421–435
- Córdoba FE, Guerra L, Rodríguez CC et al (2014) Una visión paleolimnológica de la variabilidad hidroclimática reciente en el centro de Argentina: desde la Pequeña Edad de Hielo al siglo XXI. *Latin Am J Sedimentol Basin Anal* 21(2):139–163
- Córdoba FE, Piovano EL, Guerra L et al (2017) Independent time markers validate ²¹⁰Pb chronologies for two shallow Argentine lakes in Southern Pampas. *Quat Int*. <https://doi.org/10.1016/j.quaint.2016.07.003>
- d’Orgeville M, Peltier WR (2007) On the Pacific decadal oscillation and the Atlantic multidecadal oscillation: might they be related? *Geophys Res Lett* 34:3–7. <https://doi.org/10.1029/2007GL031584>
- De Almeida RAF, Nobre P, Haarsma RJ, Campos EJD (2007) Negative ocean–atmosphere feedback in the South Atlantic convergence zone. *Geophys Res Lett* 34(18):1–5. <https://doi.org/10.1029/2007g1030401>
- Depetris PJ (2007) The parana river under extreme flooding: a hydrological and hydro-geochemical insight. *Interciencia* 32:656–662
- Díaz GM, Ferreira LJ, Skansi MM (2013) Estudio de la relación entre el nivel de la napa freática y el índice de precipitación estandarizado en diferentes escalas mensuales en Argentina. V Simposio Internacional de Climatología, 15–19 September 2013 Florianópolis, SC, Brasil
- Elisio M, Vera C, Miranda Leandro A (2018) Influences of ENSO and PDO phenomena on the local climate variability can drive extreme temperature and depth conditions in a Pampean shallow

- lake affecting fish communities *Environ Biol Fish* 101:1–14. <https://doi.org/10.1007/s10641-018-0726-2>
- Enfield DB, Mestas-Nunez AM, Trimble PJ (2001) The Atlantic multidecadal oscillation and its relationship to rainfall and river flows in the continental US. *Geophys Res Lett* 28:2077–2080
- Folland CK, Parker DE, Colman AW, Washington R (1999) Large scale modes of ocean surface temperature since the late nineteenth century. In: Navarra A (ed) *Beyond El Niño*. Springer, Berlin, Heidelberg, pp 73–102
- Garreaud R, Battisti DS (1999) Interannual (ENSO) and Interdecadal (ENSO-like) variability in the Southern hemisphere tropospheric circulation. *J Clim* 12(7):2113–2123
- Garreaud RD, Vuille M, Compagnucci R, Marengo J (2009) Present-day South American climate. *Palaeogeogr Palaeoclimatol Palaeoecol* 281:180–195. <https://doi.org/10.1016/j.palaeo.2007.10.032>
- Gatti S (2010) Melincué, su historia. Biblioteca Popular Bernardino Rivadavia. Melincué, Santa Fe, Argentina
- Giese BS, Urizar SC, Fuc NS (2002) Southern hemisphere origins of the 1976 climate shift. *Geophys Res Lett* 29(2):1014. <https://doi.org/10.1029/2001GL013268>
- Giorgi F (2002) Variability and trends of sub-continental scale surface climate in the twentieth century. Part I: observations. *Clim Dyn* 18:675–692. <https://doi.org/10.1007/s00382-001-0204-x>
- Guerra L (2015) Registros de la variabilidad hidroclimática del Holoceno tardío en la Llanura Pampeana Argentina: Limnogeología de la laguna Melincué. Ph.D. thesis, University of Cordoba, Argentina, p 222
- Guerra L, Piovano EL, Córdoba FE et al (2015) The hydrological and environmental evolution of shallow Lake Melincué, central Argentinean Pampas, during the last millennium. *J Hydrol*. <https://doi.org/10.1016/j.jhydrol.2015.01.002>
- Guerra L, Piovano EL, Córdoba FE et al (2017) Climate change evidences from the end of the Little Ice Age to the Current Warm Period registered by Melincué Lake (Northern Pampas, Argentina). *Quat Int*. <https://doi.org/10.1016/j.quaint.2016.06.033>
- Harris I, Jones PD, Osborn TJ, Lister DH (2014) Updated high-resolution grids of monthly climatic observations—the CRU TS3.10 dataset. *Int J Climatol* 34:623–642. <https://doi.org/10.1002/joc.3711>
- Hijmans RJ, Cameron SE, Parra JL et al (2005) Very high resolution interpolated climate surfaces for global land areas. *Int J Climatol* 25:1965–1978. <https://doi.org/10.1002/joc.1276>
- Hipel KW, McLeod AI (1994) Time series modelling of water resources and environmental systems, vol 45. Elsevier, Amsterdam
- Huang HP, Seager R, Kushnir Y (2005) The 1976/77 transition in precipitation over the Americas and the influence of tropical sea surface temperature. *Clim Dyn* 24:721–740. <https://doi.org/10.1007/s00382-005-0015-6>
- IPCC (2014) Climate change 2013—the physical science basis: working group I contribution to the fifth assessment report of the intergovernmental panel on climate change. Cambridge University Press, Cambridge
- Iriondo M (1989) Quaternary lakes of Argentina. *Palaeogeogr Palaeoclimatol Palaeoecol* 70:81–88. [https://doi.org/10.1016/0031-0182\(89\)90081-3](https://doi.org/10.1016/0031-0182(89)90081-3)
- Iriondo M, Kröhling D (2007) Geomorfología y sedimentología de la cuenca superior del río Salado (sur de Santa Fe y noroeste de Buenos Aires, Argentina). *Latin Am J Sediment Basin Anal* 14(1):1–23
- Jacques-Coper M, Garreaud RD (2015) Characterization of the 1970s climate shift in South America. *Int J Climatol* 35:2164–2179. <https://doi.org/10.1002/joc.4120>
- Kayano MT, Capistrano VB (2014) How the Atlantic multidecadal oscillation (AMO) modifies the ENSO influence on the South American rainfall. *Int J Climatol* 34:162–178. <https://doi.org/10.1002/joc.3674>
- Kayano MT, Pestrelo de Oliveira C, Andreoli RV (2009) Interannual relations between South American rainfall and tropical sea surface temperature anomalies before and after 1976. *Int J Climatol* 29:1439–1448
- Kreimer R (1969) Descripción Hidrogeológica de la Zona de Firmat-Casilda y Cañada de Gómez. Provincia de Santa Fe. Dirección Nacional de Geología y Minería
- Krishnamurthy V, Misra V (2010) Observed ENSO teleconnections with the South American monsoon system. *Atmos Sci Lett* 11:7–12. <https://doi.org/10.1002/asl.245>
- Kröhling DM (1999) Upper quaternary geology of the lower Carcarañá Basin, North Pampa, Argentina. *Quat Int* 57:135–148
- Leroy SAG, Warny S, Lahijani H, Piovano EL, Fanetti D, Berger AR (2010) The role of geosciences in the mitigation of natural disasters: five case studies. Springer, Dordrecht, pp 115–147
- Mantua NJ, Hare SR (2002) The Pacific decadal oscillation. *J Oceanogr* 58(1):35–44
- Mantua NJ, Hare SR, Zhang Y, et al (1997) A Pacific interdecadal climate oscillation with impacts on salmon production. *Bull Am Meteorol Soc* 78:1069–1079. [https://doi.org/10.1175/1520-0477\(1997\)078%3C1069:APICOW%3E2.0.CO;2](https://doi.org/10.1175/1520-0477(1997)078%3C1069:APICOW%3E2.0.CO;2)
- Meehl GA, Hu A, Arblaster JM, Fasullo J, Trenberth KE (2013) Externally forced and internally generated decadal climate variability associated with the interdecadal Pacific oscillation. *J Clim* 26:7298–7310
- Miller A, Cayan D, Barnett T, Graham N, Oberhuber J (1994) The 1976–77 climate shift of the Pacific ocean. *Oceanography* 7(1):21–26
- Morales MS, Carilla J, Grau HR, Villalba R (2015) Multi-century lake area changes in the Southern Altiplano: a tree-ring-based reconstruction. *Clim Past* 11:1139–1152. <https://doi.org/10.5194/cp-11-1139-2015>
- Newman M, Alexander MA, Ault TR, Cobb KM, Deser C, Di Lorenzo E, Mantua NJ, Miller AJ, Minobe S, Nakamura H, Schneider N, Vimont DJ, Phillips A, Scott JD, Smith CA (2016) The Pacific decadal oscillation, revisited. *J Clim* 29(12):4399–4427
- Paegle JN, Mo KC (2002) Linkages between summer rainfall variability over South America and sea surface temperature anomalies. *J Clim* 15(12):1389–1407
- Palamedi S (2006) El Registro del cambio climático en la Región Pampeana Argentina, la Laguna Melincué. Trabajo Final de Grado. Escuela de Geología, FCEFyN, UNC, inédito
- Pasotti P, Albert OA, Canoba CA (1984) Contribución al conocimiento de la Laguna Melincué. Publicaciones del Instituto de Fisiografía y Geología 66:1–31
- Pasquini AI, Depetris PJ (2010) ENSO-triggered exceptional flooding in the Paraná River: where is the excess water coming from? *J Hydrol* 383(3):186–193
- Pasquini AI, Lecomte KL, Piovano EL, Depetris PJ (2006) Recent rainfall and runoff variability in central Argentina. *Quat Int* 158:127–139. <https://doi.org/10.1016/j.quaint.2006.05.021>
- Penalba OC, Vargas WM (2004) Interdecadal and interannual variations of annual and extreme precipitation over central-northeastern Argentina. *Int J Climatol* 24(12):1565–1580
- Penalba OC, Rivera JA, Pántano VC (2014) The CLARIS LPB database: constructing a long-term daily hydro-meteorological dataset for La Plata Basin, Southern South America. *Geosci Data J* 1(1):20–29
- Peralta E (2003) Propuesta para la planificación del manejo sustentable de la cuenca hidrográfica y de aporte directo de la Laguna Melincué. Reportes técnicos de la Facultad de Ingeniería (Universidad Nacional de Rosario) 3:1–70
- Peralta EP (2017) Ordenamiento territorial ambiental de la cuenca hidrográfica y de aporte directo a la Laguna Melincué. *Boletín*

- del Instituto de Fisiografía y Geología 87:23–34 (**Rosario, 10-11-2017. ISSN 1666-115X**)
- Piovano EL, Ariztegui D, Moreiras SD (2002) Recent environmental changes in Laguna Mar Chiquita (central Argentina): a sedimentary model for a highly variable saline lake. *Sedimentology* 49:1371–1384. <https://doi.org/10.1046/j.1365-3091.2002.00503.x>
- Piovano EL, Larizzatti FE, Fávoro DI, Oliveira SM, Damatto SR, Mazzilli BP, Ariztegui D (2004) Geochemical response of a closed-lake basin to 20th century recurring droughts/wet intervals in the subtropical Pampean Plains of South America. *J Limnol* 63(1):21–32
- Piovano EL, Ariztegui D, Córdoba F, Cioccale M, Sylvestre F (2009) Hydrological variability in South America below the Tropic of Capricorn (Pampas and eastern Patagonia, Argentina) during the last 13.0 ka. In: Vimeux F, Sylvestre F, Khodri M (eds) Past climate variability from the last glacial maximum to the Holocene in South America and surrounding regions: from the last glacial maximum to the Holocene. Springer, Berlin, pp 323–351
- Quiros R, Drago E (1999) The environmental state of Argentinean lakes: an overview. *Lakes Reserv Res Manag* 4:55–64. <https://doi.org/10.1046/j.1440-1770.1999.00076.x>
- Quiros R, Renella AM, Boveri MB et al (2002) Factores que afectan la estructura y el funcionamiento de las lagunas pampeanas. *Ecol Austral* 12:175–185
- Robertson AW, Mechoso CR (1998) Interannual and decadal cycles in river flows of southeastern South America. *J Clim* 11(10):2570–2581
- Romano M, Barberis I, Pagano F, Maidagan J (2005) Seasonal and interannual variation in waterbird abundance and species composition in the Melincué saline lake, Argentina. *Eur J Wildl Res* 51(1):1–13
- Romano M, Barberis I, Guerra L, Piovano E, Minotti P (2014) Sitio Ramsar Humedal Laguna Melincué: estado de situación. Acosta Hermanos, Santa Fe. ISBN 978-987-45488-0-1
- Russián G, Agosta E, Compagnucci R (2015) Variaciones en baja frecuencia de la precipitación estacional en la región Pampa amarilla y posibles forzantes. *Meteorologica* 40(1):17–42
- Scarpati OE, Capriolo AD (2013) Sequías e inundaciones en la provincia de Buenos Aires (Argentina) y su distribución espacio-temporal. *Investigaciones Geográficas Boletín del Instituto de Geografía* 2013(82):38–51
- Schneider CA, Rasband WS, Eliceiri KW (2012) NIH Image to ImageJ: 25 years of image analysis. *Nat Methods* 9:671–675
- Seager R, Naik N, Baethgen W, Robertson A, Kushnir Y, Nakamura J, Jurburg S (2010) Tropical oceanic causes of interannual to multi-decadal precipitation variability in southeast South America over the past century. *J Clim* 23(20):5517–5539
- Silio-Calzada A, Barquín J, Huszar VL, Mazzeo N, Méndez F, Álvarez-Martínez JM (2017) Long-term dynamics of a floodplain shallow lake in the Pantanal wetland: is it all about climate? *Sci Total Environ* 605:527–540
- Stutz S, Borel CM, Fontana SL, Tonello MS (2012) Holocene changes in trophic states of shallow lakes from the Pampa plain of Argentina. *Holocene* 22:1263–1270. <https://doi.org/10.1177/0959683612446667>
- Taschetto AS, Wainer I (2008) Reproducibility of South American precipitation due to subtropical South Atlantic SSTs. *J Clim* 21(12):2835–2851
- Ting M, Kushnir Y, Seager R, Li C (2009) Forced and internal twentieth-century SST trends in the North Atlantic. *J Clim* 22(6):1469–1481
- Torrence C, Compo G (1998) A practical guide to wavelet analysis. *Bull Am Meteorol Soc* 79(1):61–78
- Trenberth KE (1990) Recent observed interdecadal climate changes in the Northern Hemisphere. *Bull Am Meteorol Soc* 71(7):988–993
- Troin M, Vallet-Coulomb C, Sylvestre F, Piovano E (2010) Hydrological modelling of a closed lake (Laguna Mar Chiquita, Argentina) in the context of 20th century climatic changes. *J Hydrol* 393(3):233–244
- Troin M, Vrac M, Khodri M et al (2016) A complete hydro-climate model chain to investigate the influence of sea surface temperature on recent hydroclimatic variability in subtropical South America (Laguna Mar Chiquita, Argentina). *Clim Dyn* 46:1783–1798. <https://doi.org/10.1007/s00382-015-2676-0>
- Venencio MV, García NO (2011) Interannual variability and predictability of water table levels at Santa Fe Province (Argentina) within the climatic change context. *J Hydrol* 409(1–2):62–70
- Vera C, Higgins W, Amador J, Ambrizzi T, Garreaud R, Gochis D, Gutzler D, Lettenmainer D, Marengo J, Mechoso CR, Nogues-Paegle J, Silva Dias PL, Zhang C (2006) Toward a unified view of the American monsoon system. *J Clim* 19:4977–5000. <https://doi.org/10.1175/jcli3896.1>
- Vicente-Serrano SM, Beguería S, López-Moreno JI (2010) A multi-scale drought index sensitive to global warming: the standardized precipitation evapotranspiration index. *J Clim* 23:1696–1718. <https://doi.org/10.1175/2009JCLI2909.1>
- Vuille M, Burns SJ, Taylor BL et al (2012) A review of the South American monsoon history as recorded in stable isotopic proxies over the past two millennia. *Clim Past* 8:1309–1321. <https://doi.org/10.5194/cp-8-1309-2012>
- Zhou J, Lau K-M (1998) Does a monsoon climate exist over South America? *J Clim* 11:1020–1040
- Zhou J, Lau KM (2001) Principal modes of interannual and decadal variability of summer rainfall over South America. *Int J Climatol* 21(13):1623–1644
- Zimmermann ED, Riccardi GA, Arraigada M, Pieroni H (2000) Generación de series de lluvias medias areales. Erik D. Zimmermann, Gerardo A. Riccardi, Martín Arraigada, Horacio Pieroni

Publisher's Note Springer Nature remains neutral with regard to jurisdictional claims in published maps and institutional affiliations.